Experimental investigation of optically gain-clamped EDFAs in dynamic optical-burst-switched networks

Benjamin J. Puttnam,[1,*] Benn C. Thomsen,[1] Alicia Lopez,[2] and Polina Bayvel[1]

[1]*Optical Networks Group, University College London, Torrington Place, London, WC1E7JE, UK*
[2]*Photonic Technologies Group, i3A, University of Zaragoza, María de Luna 1, 50018 Zaragoza, Spain*
[*]*Corresponding author: bputtnam@ee.ucl.ac.uk*

Received July 23, 2007; revised November 19, 2007; accepted November 20, 2007; published January 15, 2008 (Doc. ID 85535)

An experimental investigation of optically gain-clamped Er-doped fiber amplifiers (EDFAs) for application in dynamic burst-switched networks is presented. We characterize the performance of optically gain-clamped EDFAs, in terms of the signal quality of surviving channels with respect to input power variations, as a function of the feedback cavity loss. This is carried out for both a single EDFA as well as cascaded EDFAs in a realistic network scenario, where bursts are asynchronously added and dropped at each node. We show that the optimum feedback cavity loss is not only a function of input power fluctuation and feedback wavelength but also the number of hops through the network. © 2008 Optical Society of America

OCIS codes: 250.4480, 060.4250.

1. Introduction

Optical burst switching (OBS) is a key technology for the next generation of dynamically reconfigurable optical networks that are able to adapt in response to changing traffic demand [1]. In addition to tunable wavelength burst transmitters [2] and optical receivers capable of accurately recovering the timing information and data from asynchronous optical bursts of variable power [3], these networks require optical amplification that is insensitive to rapidly changing input powers ranging from zero to saturation. Due to its broad gain spectrum, polarization insensitivity, and slow gain dynamics, the Er-doped fiber amplifier (EDFA) is now the standard for all point-to-point WDM systems. However, since the total output power of a saturated EDFA is broadly constant, input power fluctuations, caused by adding and dropping bursts, induce gain transients on surviving channels that lead to transmission penalties. The power variations across a burst arising from EDFA gain transients are particularly problematic in standard burst mode receivers, which employ a fixed decision threshold [4] and can also lead to potentially catastrophic failure of downstream components.

A number of techniques using either optical feedback or electronic control have been proposed to ensure constant gain after adding and dropping of channels in WDM systems and dynamic burst switched networks, where bursts may be added and dropped asynchronously at each node. Electronic techniques use a photodiode to detect incoming power variations followed by a control circuit to adjust the power of a compensating dummy channel [5,6] or vary the power of the pump to control the gain of the remaining signals [7–9].

In this paper we investigate the performance of an all-optically gain-clamped EDFA (GC-EDFA) [10], where a portion of amplified spontaneous emission (ASE) from the EDFA output is coupled back to the input to form a laser cavity. This clamps the gain of each channel as the power of the lasing channel is able to adjust to input power fluctuations. This technique has the advantage that high speed electronics, additional lasers, and photodiodes are not required. In the ring laser configuration used here, first described in [10], gain clamping is achieved by using a bandpass filter to select the lasing wavelength, and a variable attenuator to adjust the feedback cavity loss

(FCL), which controls the level of gain compression. Fiber Bragg gratings (FBGs) may also be used to select the lasing wavelength and block transmission of the feedback wavelength with the output signal channels [11]; however, from an experimental point of view this configuration is less flexible and is not investigated here.

Previous work on all-optical gain-clamping has focused on reducing the magnitude of the principle gain transients, that is, relaxation oscillations (ROs), and steady state power fluctuations (SSPFs) in the high gain compression regime [12] but without considering the impact that these effects have on the bit error rate (BER) at the receiver. BER measurements of transmitted signals were used to study RO resonance effects in [13] but not to optimize the optical feedback cavity design. Here, we build on the theoretical work of Richards *et al.* [14] and experimentally assess the effect that these transients have on the signal quality in terms of BER as the gain compression varies from high to zero in a cascade of GC-EDFAs.

The paper is arranged as follows. In Section 2 we describe the operating principle and theory of all-optical gain-clamping. In Section 3 we show that for a single amplifier an optimum value of FCL exists and that this value is dependent on both the magnitude of the input power fluctuations (number of added/dropped bursts) and the feedback cavity wavelength. This optimum point is quantified in terms of both the magnitude of the transients, as in previous work, and the BER. Section 4 presents the results obtained using a dynamic optical network testbed based on a recirculating transmission loop to assess the performance of multiple cascaded GC-EDFAs. In particular we consider a cascade of GC-EDFAs where bursts are added and dropped at each routing node such that impairments caused by gain transients are introduced at each node and accumulate on bursts that traverse the entire end-to-end path as would be the case in a reconfigurable network. This differs from previous studies of cascaded GC-EDFAs in point-to-point links, which only considered the effect of burst add and drop at the beginning of a cascade of amplifiers with gain-clamping on all amplifiers [14,15] or where only the first amplifier of the chain is gain-clamped [14,16].

2. Principle of Optical Gain-Clamping

Add/drop events in dynamic networks cause power transients at the input to EDFAs, which in turn result in cross-gain-modulation on the remaining channels. Without optical feedback, this effect appears as SSPFs as shown in Fig. 1 at the maximum FCL. The temporal response of the SSPF depends on the EDFA carrier lifetime and is of the order of 100 μs. With sufficient optical feedback to maintain lasing at the feedback wavelength, the gain of the signal channels is clamped, thereby suppressing the

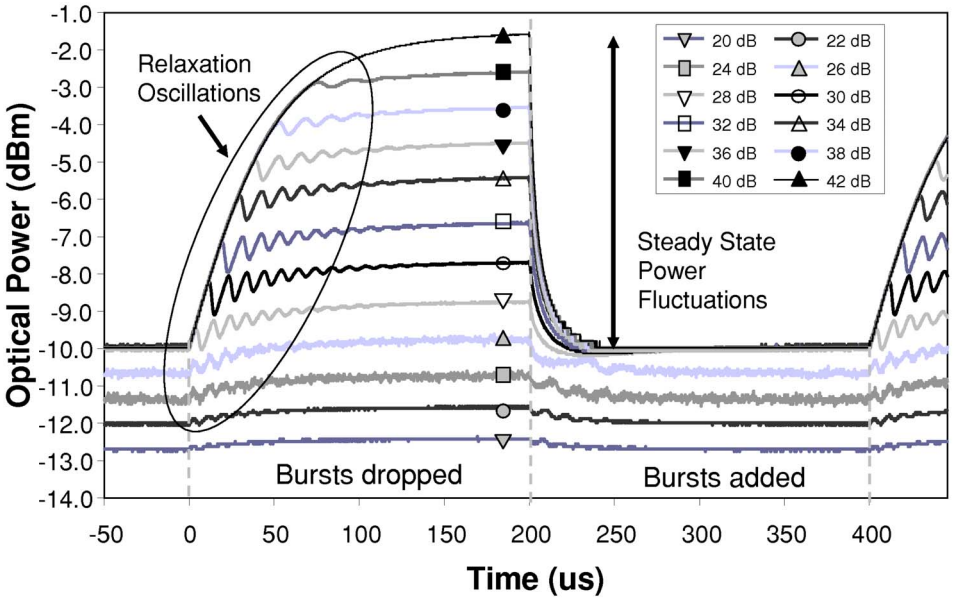

Fig. 1. SSPFs and ROs on probe channel as a function of feedback cavity loss caused by burst add/drop (16 simultaneous bursts).

SSPFs. As shown in [10] if the lasing condition is met, then under steady state conditions and homogeneous broadening the dependence of the kth signal channel gain (G_k) on the FCL is given by Eq. 2 in [10],

$$G_k = \exp\left[-\alpha_k L + \frac{P_f^{\mathrm{IS}}}{P_f^{\mathrm{IS}}}(\ln \beta + \alpha_f L) \right],$$

where $\beta = 1/\mathrm{FCL}$, P_f^{IS} and P_k^{IS} are the intrinsic saturation powers, and α_f and α_k are the absorption coefficients of the feedback and kth channel, respectively, and L is the doped fiber length. This equation shows that the gain of any signal channel is independent of the total optical input power, for the range of input powers for which lasing is possible, and that the gain of each channel depends on the FCL. In practice, the FCL and EDFA pump power are adjusted to ensure that the gain at the feedback wavelength is just above the lasing threshold at maximum input signal power.

Thus, the FCL is the most important control parameter for dynamic network operation since its value determines the trade-off between maximizing the gain transient suppression and the gain seen by the propagating signals. Reducing the power in the feedback channel by increasing feedback cavity losses increases the amount of gain available to signal channels but limits the magnitude of input power variations for which lasing, and hence transient suppression, is achieved. Thus, there is an optimum point at which effective transient suppression is achieved while maintaining a large gain.

The use of optical feedback also introduces additional amplitude fluctuations due to ROs associated with the laser cavity [12,14]. The RO frequency depends on the feedback cavity length and the photon and carrier lifetimes. The RO frequency is of the order of 50–100 kHz for the feedback cavity used here. Under optical feedback there is also a small static contribution to the output power fluctuations from spectral hole burning (SHB), arising from an inhomogeneity in the Er gain spectrum, that varies with the optical feedback wavelength [12]. However, we find these two effects to be small in comparison to the SSPF, which is the dominant signal degradation mechanism.

3. Performance of a Single GC-EDFA

The experimental setup for assessing the performance of a single GC-EDFA, shown schematically in Fig. 2, was based on an experimental model of an OBS link between two core routers containing a single GC-EDFA with a feedback wavelength of λ_F. Measurements to quantify the effect of burst add/drop on a surviving channel were made on a continuous probe channel at wavelength (λ_P) from edge router 1. Meanwhile, edge router 3 generated an ON–OFF burst sequence at wavelength (λ_B) that simulated the adding and dropping of multiple simultaneous bursts. The probe and burst channels were transmitted across the link containing the GC-EDFA and dropped at the second core router to allow reception of the probe channel at edge router 2.

The probe channel (Tx_1), shown in Fig. 3, was modulated with a nonreturn-to-zero (NRZ) 10 Gbit/s pseudo random binary sequence (PRBS) of length $2^{15}-1$. The burst channel (Tx_2) was based on a multisection semiconductor tunable laser [2] switched between two wavelengths (1535 and 1540 nm) with a period of 400 μs, 50% duty cycle, and 100 ns switching time. This was coupled into the link amplifier via a wavelength routing node, which only routed λ_B at 1535 nm to the GC-EDFA. The burst length of

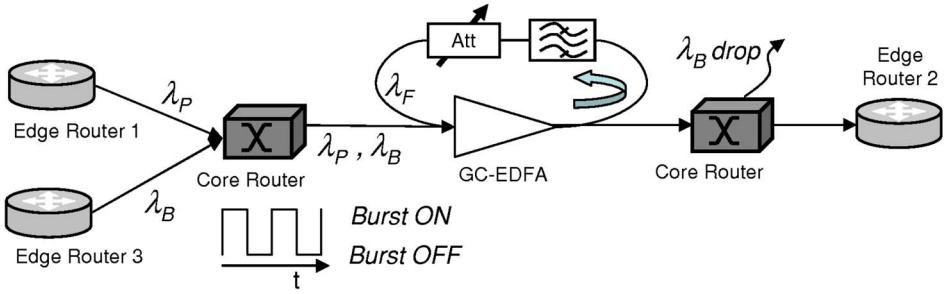

Fig. 2. OBS link schematic for single GC-EDFA analysis.

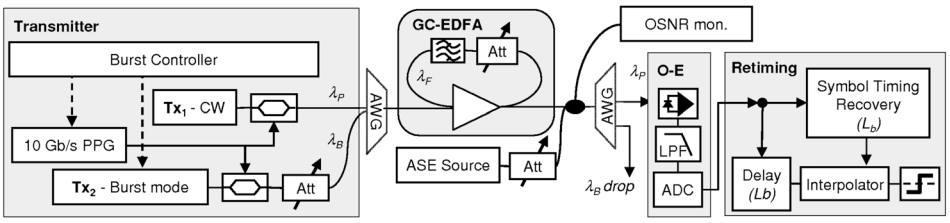

Fig. 3. Experimental burst mode transmitter, GC-EDFA, and digital optical receiver architecture.

200 μs was chosen to be of the order of that envisaged for Type II OBS dynamic optical networks [1] and also matched to the time scale of the EDFA transients [14]. The power of the burst channel, Tx_2, was varied to replicate the impact of different numbers of added/dropped bursts up to a maximum of 16 bursts. This corresponds to a power difference of 12 dB compared to the probe channel power of −17 dBm at the EDFA input. The transmitter setup and timing was designed to replicate the worst case network scenario, with a single surviving channel and multiple bursts added and dropped simultaneously.

The GC-EDFA was operated with a constant pump power and gain-clamped using a feedback loop based on a 13 dB tap at the EDFA output, an optical bandpass filter (0.4 nm 3 dB bandwidth) to select the feedback wavelength, a variable optical attenuator (VOA) to control the FCL, and a 3 dB coupler to couple the feedback channel and signal together at the EDFA input. The minimum FCL was 20 dB due to the insertion loss of the couplers and components in the feedback loop.

The signals were received using a digital optical receiver consisting of a 10 Gbit/s direct-current (DC) coupled photodiode and 7 GHz fourth order low pass Bessel filter, followed by an asynchronous 20 GS/s analog to digital converter (ADC). Symbol timing [17] and data recovery [18] was implemented offline using software based digital signal processing (DSP). To measure the probe channel BER, the digital receiver captured a single cycle of the burst add/drop sequence and was operated with a fixed decision threshold optimized to deliver the best BER performance across the entire 400 μs data sequence. To allow for error counting over the limited sequence length, noise from an ASE noise source was added before the receiver to obtain a fixed optical signal-to-noise ratio (OSNR) of 11 dB (0.1 nm resolution).

To identify how each of the degradation effects affect the signal quality of the surviving channel with bursty input traffic, measurements of both SSPFs and ROs were made on the burst envelope as a function of FCL for each feedback wavelength and number of dropped channels. Figure 1 shows the received waveforms for cavity losses ranging from 20–42 dB measured using a low-speed photodiode and digital oscilloscope. The feedback wavelength used was 1528 nm, and the burst channel power variation of 12 dB was equivalent to 16 simultaneously added and dropped bursts. The range of FCL causes gain compression at the probe channel wavelength of 1542.6 nm ranging from 0–12 dB with only the probe channel present (burst dropped) and 0–3 dB with all channels present (bursts added). Since a realistic network would be dimensioned for the case with all channels present, the gain compression value with all channels present (up to 3 dB) represents the maximum gain compression at the minimum FCL in a system of up to 17 channels.

With the FCL minimized to the component insertion loss the feedback channel is able to maintain enough power to almost completely suppress both SSPFs and ROs on the probe channel caused by the simultaneous adding and dropping of 16 bursts. However, this is at the expense of reduced small-signal gain for the probe channel, which suffers a gain compression of 3 dB compared to an unclamped operation with all channels present. As the power in the feedback channel is reduced with increasing FCL, the small-signal gain increases, and both impairments begin to appear on the probe channel. When the FCL exceeds 26 dB there is insufficient gain in the feedback channel for the lasing condition to be satisfied when the burst channel is present, and this results in the sharp increase in SSPFs. A further increase in FCL results in additional SSPF until the feedback channel is unable to laze for both burst add and drop events and the EDFA gain is no longer clamped. This occurs for a FCL of 42 dB in Fig. 1. Relaxation oscillations reach a peak in both amplitude and frequency between these last two stages. As shown in [14], variations in the power of the feedback channel also

change the gain balance of signal channels (gain tilt) and the noise figure. Over the range of feedback powers investigated, with a feedback wavelength of 1528 nm, the maximum change in gain between the probe and burst channels was 0.9 dB, equivalent to a change in gain tilt of 0.12 dB/nm. For the amplifier used in these experiments the noise figure without optical feedback is 5.1 dB, and this increases by 0.5 dB at maximum gain compression.

To identify the optimum FCL, BER measurements of the received bursts were used to calculate the Q-factor of the probe channel transmitted through the GC-EDFA with periodic burst add/drop as a function of the FCL. Figure 4(a) shows Q-factor penalty versus FCL for the probe channel when three bursts are simultaneously added and dropped at 200 μs intervals. The Q-factor penalty is minimized at a FCL of 30 dB and increases for both lower and higher values of FCL. At low FCLs, a Q-factor penalty compared to the optimum value is observed because of the reduced signal gain due to excess power in the feedback channel. At high FCL, the Q-factor penalty increases due to both SSPFs and ROs as the feedback channel now possesses insufficient power to clamp the gain of the probe channel and it becomes susceptible to input power fluctuations from burst add and drop.

Figure 4(b) shows the correlation between the Q-factor penalty and the measured SSPFs when 1, 3, and 16 bursts are added and dropped with a feedback wavelength of 1528 nm. In each case the required FCL for the minimum Q-factor penalty, at around 32, 30, and 26 dB for 1, 3, and 16 bursts, respectively, corresponds to the onset point for the SSPF. This highlights the trade-off between the amplifier gain and transient suppression. As the number of burst channels added and dropped increases, the required FCL for optimum performance reduces as more gain in the feedback channel is required to suppress the increasing input power fluctuations. It is also noted that the onset of ROs occurs for a FCL of 26, 24, and 20 dB for 1, 3, and 16 bursts, respectively. In each case, this is in the region where a negligible Q-factor penalty is observed. This, and the high correlation between the Q-factor penalty and SSPFs shown in Fig. 4(b), shows that SSPF is the dominant signal degradation mechanism when there is insufficient power in the lasing channel to compensate for input power fluctuations.

Figure 4 shows that for a specific input power fluctuation, an optimum FCL may be set to balance the penalty caused by reduced gain at low FCL and SSPF at high FCL. How the choice of feedback wavelength affects this optimum point was then investigated by determining this optimum point as a function of feedback wavelength. Previously in [12], the wavelength dependence of ROs and SSPFs caused by SHB has been studied for GC-EDFAs with high gain compression. In this paper, we are concerned with how the choice of feedback wavelength affects the BER of propagating channels with the gain compression minimized by control of the FCL. For a series of feedback wavelengths across the EDFA gain band we found little or no variation in the absolute value of the optimum Q-factor for each burst channel power variation, but the FCL loss for which the optimum Q-factor value occurred was dependent on the feedback wavelength due to gain variations across the EDFA gain spectrum. Thus we find that selecting a feedback wavelength on or close to the gain peak, in this case just outside the C-band at 1528 nm, requires the least optical feedback, and thereby maximizes the amplifier gain for propagating signal channels. Additionally, use of the gain peak

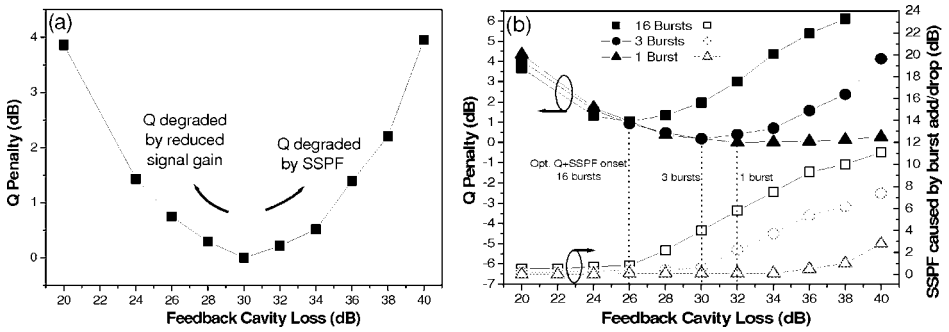

Fig. 4. (a) Q-factor penalty of surviving channel after three burst add/drop versus FCL, and (b) Q-factor penalty (solid markers) and SSPF (hollow markers) of surviving channel for 1, 3, and 16 burst add/drop for a feedback wavelength of 1528 nm.

for the feedback wavelength, which should be filtered from the amplifier output, allows for the entire *C*-band and flat region of the gain spectrum to be used for burst signal amplification.

Once the feedback wavelength is selected the results in Fig. 4 show that the optical feedback cavity design is dependent on the maximum range of the input power fluctuations that must be accommodated. This power range is determined by network considerations such as the number of wavelengths in use or the router port count. This, in turn, sets the FCL, which should be minimized while ensuring the feedback channel is able to laze with all channels present.

4. Performance of Cascaded GC-EDFA

In a dynamic burst-switched network, bursts may be added and dropped asynchronously at all nodes. In order to emulate this, a recirculating transmission loop was used to set up a multihop end-to-end OBS link as shown schematically in Fig. 5.

The experimental implementation was based on a single core node with recirculating transmission as shown in Fig. 6. The transmission link is comprised of 40 km of standard single-mode fiber (SMF) fully compensated for by an additional 7 km of dispersion compensating fiber (DCF) with a total span loss of 13.5 dB. As with the single amplifier measurements the probe channel was generated from Tx_1 at λ_P (1542.6 nm) and was modulated with a 10 Gbit/s NRZ PRBS of length $2^{15}-1$. This was transmitted through a specified number of routers, GC-EDFAs, and fiber transmission stages in bursts of 250 μs, set by the loop round trip time, before being received by a digital receiver (Rx_1) at the egress edge router. The add/drop channel (λ_B) from Tx_2 was an ON–OFF burst signal at a wavelength of 1535 nm. To ensure a complete cycle fitted within the transmitted burst length the switching period was reduced to 200 μs with a 50% duty cycle. The optical power of the burst add/drop channel was set to exceed the probe channel by 9 dB to emulate the effect of eight copropagating bursts of equal power being added or dropped, simultaneously. The span EDFA was optically gain-clamped as in the single amplifier measurements with a minimum cavity loss of 20 dB and a variable attenuator to control the FCL. As shown in Section 3, the best GC-EDFA performance is obtained by exploiting the natural EDFA gain peak, hence, a feedback wavelength (λ_F) of 1528 nm was used for all measurements.

The core router comprised two $1\times N$ 100 GHz spaced arrayed waveguide gratings (AWGs). These performed the wavelength routing functionality, dropping the bursts at λ_B, while forwarding the bursts at λ_P on to the next core node, before adding new bursts at λ_B. To compensate for the additional loop and router component losses the core router contained an additional EDFA. This was placed between the drop and add ports, where only the low power (–21 dBm) continuous probe channel at wavelength λ_P propagates, and was operated in the linear regime. Operating in the linear regime ensures that there is no gain saturation, which might suppress the power fluctuations on the probe that we wish to measure and removes the requirement for gain-clamping in this amplifier.

The impact of the FCL on an end-to-end path comprising multiple GC-EDFAs with asynchronous adding and dropping of bursts at intermediate nodes was studied by monitoring the probe channel as the number of traversed nodes was increased. This enabled the measurement of the *Q*-factor penalty arising from gain transients accumulated from multiple asynchronous burst add/drop events to find the optimal FCL for varying numbers of node hops. The same DSP-based digital receiver used in the

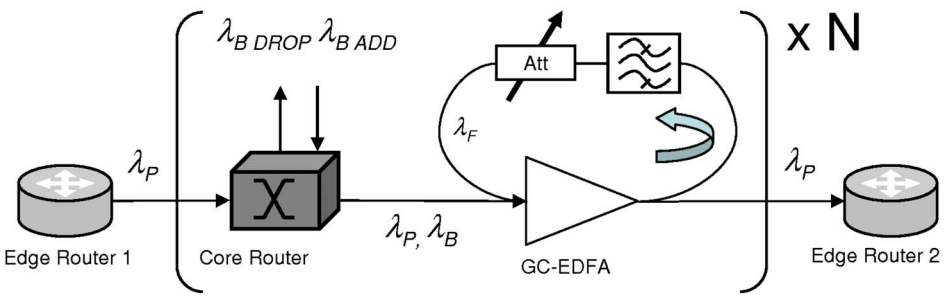

Fig. 5. OBS link representation.

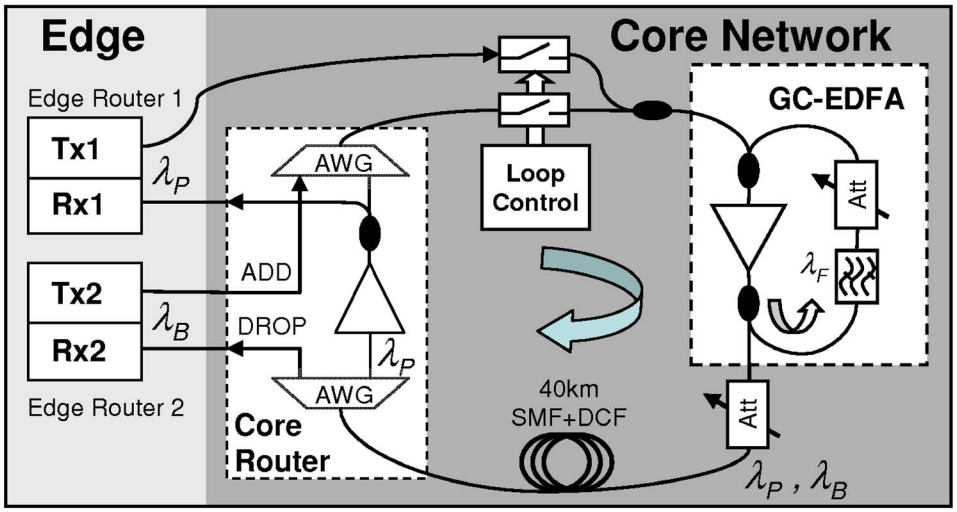

Fig. 6. Experimental setup for OBS nodes and fiber link.

single GC-EDFA measurements was used to count the number of received errors. The optimum receiver threshold was determined using the entire 250 μs loop output sequence. As with the single amplifier measurements, to allow for error counting over the limited sequence length, and to remove the degradations arising from accumulated ASE as the number of hops is increased, noise was added at the receiver to obtain a fixed OSNR of 16 dB at 0.1 nm resolution. Additionally, since increasing the FCL increases the amount of gain available to the signal channel, it was necessary to attenuate the signal to maintain a constant fiber launch power of 0 dBm to ensure operation in the linear transmission regime. The Q-factor penalty was measured as a function of FCL for 1, 5, 10, 15, 20, and 25 hops, and the results are shown in Fig. 7.

Figure 7(a) shows the Q-factor penalty for 1, 5, 15, and 25 hops and exhibits a number of important features. First, we observe a penalty as we increase the number of hops even with the FCL minimized at 20 dB, where the best transient suppression performance was obtained. This arises from small power excursions caused by the adding and dropping of bursts at each node, which are not completely suppressed, and these accumulate with the increasing number of hops. To understand the shape of the curves shown in Fig. 7(a) we must first note that the Q-factor penalty due to reduced gain at low FCL, shown in Fig. 4(a) for a single amplifier, is not seen for the cascaded results. This is an artifact of the requirement to maintain a constant fiber launch power for all measurements. Since increasing the FCL increases the amount of gain available to the signal channel it was necessary to attenuate the additional signal power in order to maintain a constant fiber launch power. A comparison of the results shown in Figs. 4(a) and 7(a) also shows that the increase in noise figure, as the FCL decreases, does not cause a significant Q-factor penalty. Had the Q-factor penalty seen in Fig. 4(a) at low FCL been the result of the increase in noise figure, then this trend

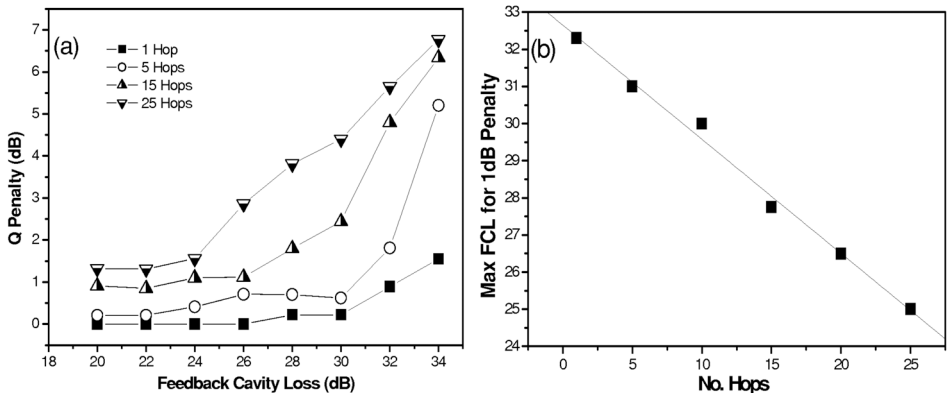

Fig. 7. Impact of FCL on Q-factor penalty with an increasing number of hops, and (b) required FCL for 1 dB penalty with an increasing number of hops.

would have also been seen in Fig. 7(a). However, in Fig. 7(a) no discernible Q-factor penalty at low FCL is seen, and thus we attribute the penalty seen in Fig. 4(a) to the reduced gain, which is compensated for in the results shown in Fig. 7(a).

What we do observe is the penalty caused by insufficient gain transient suppression as the feedback cavity losses increase, which leads to SSPFs. As shown in Fig. 4 the onset of this penalty can be used to determine the FCL required to maximize the measured Q-factor. In Fig. 7(a), we observe that the point at which this penalty starts to increase sharply due to insufficient gain transient suppression shifts to lower values of FCL as the number of hops traversed increases. This occurs because there is insufficient power in the feedback channel to compensate for the increasing amplitude fluctuations as more nodes are traversed. Thus, the transients caused by adding and dropping of bursts sharing link amplifiers accumulate with each hop, and a lower FCL is required to achieve optimum performance as the network size grows.

To quantify the amount of additional feedback required as a function of the network size, Fig. 7(b) shows the maximum required FCL for a 1 dB penalty for each value of the number of hops considered. This metric was chosen to identify the point before the penalty (caused by insufficient gain-clamping) begins to significantly degrade the BER, while maximizing the gain of the throughput signals. As described in Section 2, this may be considered to be the FCL value for optimum performance. By considering a 1 dB penalty compared to the highest measured Q-factor for each number of hops, Fig. 7(b) shows that the optimum FCL increases by approximately 0.3 dB per hop. This figure may be used to estimate the amount of additional feedback power required, above that required to meet the lasing threshold at maximum input signal power, as a function of network size.

5. Conclusion

The results of the experimental investigation show that optimum performance of an optically gain-clamped EDFA depends on the careful design of the optical feedback cavity, and that the design parameters are dependent on a number of network-wide parameters. For a given feedback wavelength and input power fluctuation, there is an optimum feedback level for which the received signal quality, quantified by the Q-factor, is maximized. Increasing the amount of optical feedback beyond the optimum, shown here by reduced FCL, reduces the Q-factor by decreasing the gain available to signal channels. Reducing the optical feedback by increasing the FCL limits the suppression of power transients caused by burst add/drop and leads to a Q-factor penalty that is also dependent on the input power change. We also showed that the dominant signal Q-factor degradation arises from SSPFs and not ROs. Our results also show that the optimum FCL is not in the region of high gain compression, which has been the focus of previous studies.

The amount of optical feedback required to suppress gain transients is dependent on the magnitude of the input power fluctuations. Hence, for a given GC-EDFA the required optical feedback is dependent on knowledge of the maximum possible input power fluctuations. This may be determined from the physical network parameters such as the port count at a preceding router or the number of wavelengths used in the network.

The optimum choice of feedback wavelength was shown to be at the 1528 nm gain peak as this minimizes the feedback power required to provide transient suppression while maximizing the gain for the signal channels. It also allows the entire C-band and the flatter part of the EDFA spectrum to be used for signal channels.

The performance of cascaded amplifiers showed that the impairments caused by insufficient optical gain-clamping accumulate across a network path. In an experimental model of an OBS network path comprising multiple routing and amplification stages with bursts asynchronously added and dropped at each hop, it is shown that additional optical feedback is required to compensate for the accumulated gain transients in propagating bursts. The accumulation of power transients was found to shift the optimal FCL by 0.3 dB per node hop. Hence, the feedback cavity design can limit the number of hops a burst is able to traverse for a specified performance metric and, hence, limit the network size.

The experimental results presented demonstrate the potential of a GC-EDFA to reduce the impact of gain transients on transmitted bursts caused by the adding and

dropping of copropagating bursts across an OBS network path. In particular, the results show that, in addition to the feedback wavelength, the optimal design of a GC-EDFA requires consideration of both the maximum possible input power variations, which may be determined by the number of wavelengths in use, and the network size.

Acknowledgments

This work was funded by EU NOBEL, Bookham Technologies: B. Thomsen is funded by an EPSRC advanced research fellowship EP/D074088/1.

References

1. P. Bayvel and M. Dueser, "Optical burst switching: research and applications," in *Proceedings of Optical Fiber Communication Conference (OFC)* (Optical Society of America, 2004), paper FO1.
2. B. Puttnam, M. Dueser, B. Thomsen, P. Bayvel, A. Bianciotto, R. Gaudino, G. Busico, L. Ponnampalam, D. Robbins, and N. Whitbread, "Burst mode operation of a DS-DBR widely tunable laser for wavelength agile system applications," in *Proceedings of Optical Fiber Communication Conference (OFC)* (Optical Society of America, 2006), Paper OW186.
3. B. C. Thomsen, B. Puttnam, and P. Bayvel, "A 10 Gb/s digital burst mode receiver," in *Optical Fiber Communication Conference (OFC)* (Optical Society of America, 2007), Paper 0ThK5.
4. K. Schneider and H. Zimmermann, "Optical burst-mode receivers for passive optical networks," in *Electron Devices for Microwave and Optoelectronic Applications (EDMO 2004)* (IEEE, 2004) pp. 60–65.
5. A. Bianciotto, A. Carena, V. Ferrero, and R. Gaudino, "EDFA gain transients: experimental demonstration of a low cost electronic control," IEEE Photon. Technol. Lett. **15**, 1351–1353 (2003).
6. A. V. Tran, C.-J. Chae, R. S. Tucker, and Y. J. Wen, "EDFA transient control based on envelope detection for optical burst switched networks," IEEE Photon. Technol. Lett. **17**, 226–228 (2005).
7. A. K. Srivastava, Y. Sun, J. L. Zyskind, and J. W. Sulhoff, "EDFA transient response to channel loss in WDM transmission system," IEEE Photon. Technol. Lett. **9**, 386–388 (1997).
8. A. Lieu, T. Cechan, and T. Naito, "Transmission and interactions of WDM burst signals in cascaded EDFAs," in *Optical Fiber Communication Conference* (Optical Society of America, 2006), paper OTuD5.
9. H. S. Chung, J. C. Lee, M. J. Chu, J. H. Lee, and H. H. Lee, "Reduction of relaxation oscillations in optical automatic gain-clamped EDFA using fast electronic feedforward," Electron. Lett. **38**, 215–217 (2002).
10. M. Zirngibl, "Gain control in EDFAs by an all-optical feedback loop," Electron. Lett. **27**, 560–561 (1991).
11. T. Subramaniam, M. A. Mahdi, P. Poopalan, S. W. Harun, and H. Ahmad, "All-optical gain-clamped erbium-doped fiber-ring lasing amplifier with laser filtering technique," IEEE Photon. Technol. Lett. **13**, 785–787 (2001).
12. G. Luo, J. L. Zyskind, J. A. Nagel, and M. A. Ali, "Experimental and theoretical analysis of RO and SHB effects in all-optical gain-clamped EDFAs for WDM networks," J. Lightwave Technol. **16**, 527–533 (1998).
13. D. H. Thomas and J. P. von der Weid, "Dynamic gain-instabilities in gain clamped EDFA," in *European Conference on Optical Communications* (ECOC, 2004), pp. 546–547.
14. D. H. Richards, J. L. Jackel, and M. A. Ali, "A theoretical investigation of dynamic all-optical automatic gain control in multichannel EDFAs and EDFA cascades," IEEE J. Sel. Top. Quantum Electron. **3**, 1027–1036 (1997).
15. M. Karasek, M. Menif, and L. A. Rusch, "Output power excursions in a cascade of EDFAs fed by multichannel burst-mode packet traffic: experimentation and modeling," J. Lightwave Technol. **19**, 933–940 (2001).
16. J. Chung and S. Y. Kim, "Dynamic performance of the all-optical gain-controlled EDFA cascade in multiwavelength add/drop networks," in *European Conference on Optical Communications* (ECOC, 1997), pp. 139–142.
17. S. J. Lee, "A new non-data-aided feedforward symbol timing estimator using two samples per symbol," IEEE Commun. Lett. **6**, 205–207 (2002).
18. F. M. Gardner, "Interpolation in digital modems—Part I: fundamentals," IEEE Trans. Commun. **41**, 501–507 (1993).